The Magnetic Field of Mars Estimated from the Data of Plasma Measurements by Soviet Artificial Satellites of Mars

K. I. Gringauz, V. V. Bezrukikh, T. K. Breus,
M. I. Verigin, and A. P. Remizov
Moscow, U.S.S.R.
Institution for Space Research

The dimensions of the obstacle forming the shock wave of Mars are estimated by use of electron trap data from Mars 2, 3, and 5. The mean altitude of the obstacle at the subsolar point can be convincingly explained if the obstacle is the magnetosphere of Mars. On the assumption that Mars has its own dipole magnetic field, the magnetic moment of Mars is estimated, $M_m \cong 2 \times 10^{22}$ gs x cm^3.

The spacecraft Mars 2, Mars 3, and Mars 5 were injected into orbit around Mars on November 27 and December 2, 1971, and on February 12, 1974, respectively. The spacecraft used identical electron traps to measure the characteristics of the electron component of the solar wind plasma, while Mars 5 also used an ion trap to measure the ionic component (ref. 1). During each revolution of these satellites around Mars, a bow shock was recorded, the existence of which was first suggested after a single fly-by of Mars by the American Mariner 4 spacecraft (ref. 2).

Figures 1a and 1b show ion spectra and electron retardation curves, respectively, for the solar wind and the transition zone behind the front of the bow shock recorded by Mars 5. We can see that both ions and electrons behind the front of the bow shock are thermalized and their concentrations increase. The characteristic changes in the spectra also serve as the criterion for determining the front of the bow shock.

The position of the front of the bow shock depends on the dimensions and form of the obstacle which stops the solar wind. Therefore, experimental determination of the position of the front of the bow shock near a planet allows us to estimate the dimensions of the obstacle and, consequently, to some extent to gain an idea of its nature.

Figure 2 shows sections of the orbits of the Mars 2, Mars 3, and Mars 5 spacecraft where they crossed the bow shock front. The characteristics of the plasma measured closest to the planet (fig. 2) are typical of the transition zone behind the bow shock (fig. 1b), while at the remotest points the measurements are characteristic of solar wind undisturbed by a planet (fig. 1a). The length of the orbital sections shown depends on the mode of operation of the instrument (2, 10, or 20 minutes) and the rate of movement of the satellite in orbit. Estimates of the dimensions of the obstacle were made by calculating the position of the front of the bow shock, on the assumption that the obstacle has the form of an extended body of rotation like that of the terrestrial magnetosphere (ref. 3). The solid line in figure 2 shows the shape and dimensions of the obstacle, and the dashed line shows the position of the front of the bow shock for Mach number $M_\infty = 8$

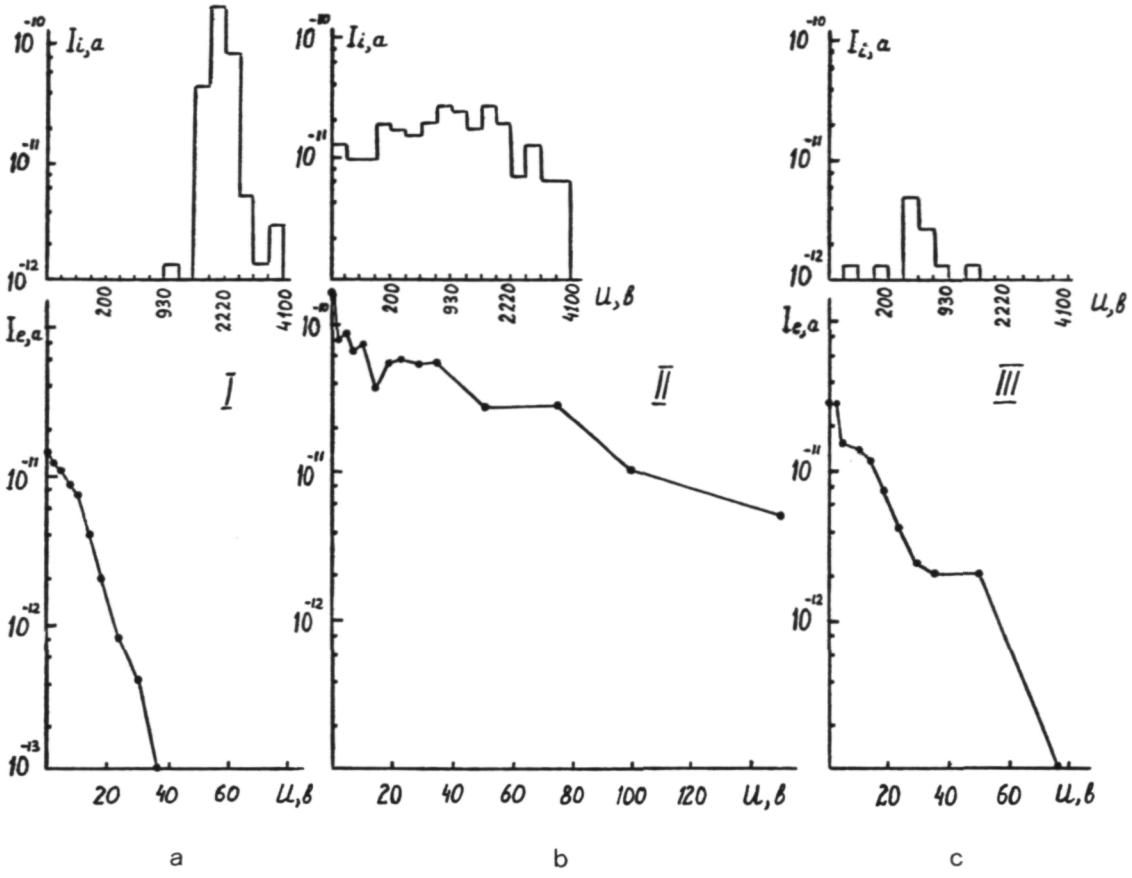

Figure 1.—*Ion spectra and electron retardation curves are shown for Mars 5 data. Figure la is for the solar wind, 1b is for the transition zone, and 1c corresponds to entry of Mars 5 into the obstacle.*

and $\gamma = 5/3$, calculated according to Spreiter and Alksne (ref. 3). The dimensions of the obstacle were selected such that the sum of squares of distances from both ends of the trajectory sectors shown in figure 2 to the front of the bow shock formed by the obstacle was minimal (ref. 4).

The areocentric distance to the subsolar point of the obstacle is $(4.6 \pm 0.8) \times 10^3$ km, and to the subsolar point of the shock wave $(5.7 \pm 1) \times 10^3$ km; or, respectively $(1.2 \pm 0.8) \times 10^3$ km and $(2.3 \pm 1) \times 10^3$ km from the surface of Mars. The relative dispersion in areocentric distances to the obstacle and shock wave front (about 17 percent) for Mars corresponds to the characteristic relative values of changes in geocentric distances to the subsolar point of the bow shock front and the magnetosphere of the Earth (about 20 percent), for example, due to changes in the dynamic pressure of the solar wind (for example, see reference 5). The high relative dispersion of the height of the obstacle and front of the bow shock above the surface of Mars is related to the fact that on Mars the dimensions of the obstacle, expressed in planetary radii, are almost an order of magnitude less than on Earth.

With the use of Mars 2 and Mars 3 data, the minimum height of the obstacle was estimated from intersection of the bow shock front by the Mars 2 spacecraft on May 12, 1972 (see fig. 2) as about 600 km. From Mars 5 to the minimum estimate of height of the obstacle is apparently about 500 km, based on intersection of the front by the spacecraft in the February 20, 1974, session

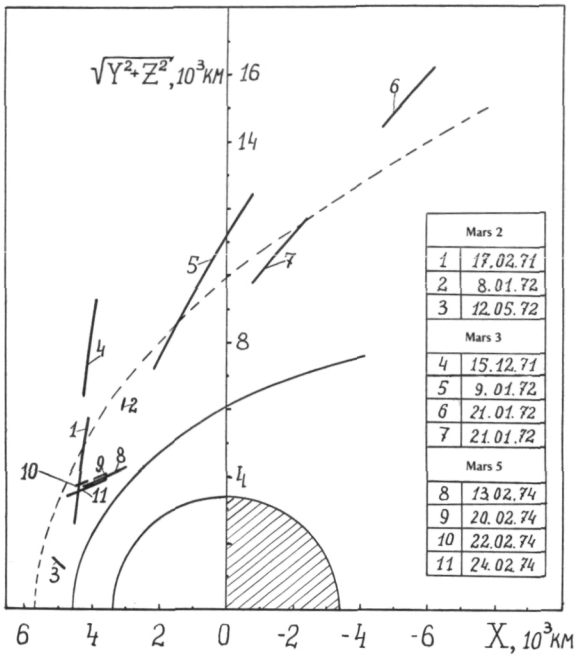

Figure 2.—*Sections of the orbits of the Mars 2, 3, and Mars 5 spacecraft are shown where they crossed the bow shock front. The length of the orbital sections depends on the mode of operation of the instrument (2, 10, or 20 min.) and the rate of movement of the satellite in orbit. The solid line shows the shape and dimensions of the obstacle, and the dashed line shows the position of the front of the bow shock for Mach number* $M_\infty = 8$ *and* $\gamma = 513$, *calculated according to Spreiter and Alksne (ref. 3).*

with 2-minute intervals between measurements. It should be noted that in the February 13, 1974, session, with 10-minute intervals between measurements, the estimate of the height of the obstacle based on the closest approach to the planet (fig. 2) yields lower values, while the estimate based on the farthest point in the trajectory sector yields higher values than in the February 20, 1974, session. However, since the dynamic pressure of the solar wind in this "10-minute" session (determined by the ion trap, with data produced before the bow shock front was intersected) was less than in the "2-minute" session of February 20, 1974, the front of the bow shock was apparently intersected on February 13, 1974, by the Mars 5 spacecraft no closer to the planet than on February 20, 1974. One confirmation of the influence of changes in dynamic solar wind pressure on the position of the bow shock front is obtained by comparison of the measurement sessions of February 20 and 22, 1974. Between these sessions the solar wind pressure decreased and, correspondingly, the boundary of the obstacle rose to an altitude of about 900 km.

The size of the obstacle determined by our data, even with its minimum size of about 500 km, does not agree with the idea that solar wind is stopped by the ionosphere of Mars (ref. 6). As follows from radio occultation (refs. 7, 8, and 9) data on the altitude distribution of electron concentrations in the ionosphere of Mars, the maximum ionospheric ionization at Mars is at about 140-km altitude; and by about 300–350 km the pressure of the Martian ionosphere is some two orders of magnitude less than the dynamic pressure of the solar wind.

Weisberg and Bogdanov (ref. 10) consider that there is an "ion cushion" (on the dayside) and a "boundary layer" (on the nightside) between the ionosphere of Mars, bounded by the ionopause, and the transition zone behind the bow shock front; and that these layers form the obstacle creating the bow shock. This boundary layer, according to Weisberg and Bogdanov (ref. 10), is formed as a result of the viscous interaction of the incident flux (that is, obviously, the flux in the transition zone behind the front of the bow shock) with particles dissipating from the ionosphere of Mars. Obviously, the pressure of particles dissipating from the ionosphere is less than the pressure within the ionosphere or at the ionopause. Weisberg and Bogdanov do not present quantitative estimates explaining how the balance of pressures at the boundary of the obstacle is realized.

The results of observations, however, can explain if the obstacle is the magnetosphere of Mars. Assuming that the primary contribution to Mars' magnetic field is made by a dipole term, we can estimate the value of the magnetic moment of Mars using the following formula (ref. 3): $M_m = D^3$

$\sqrt{2\pi k \rho_\infty V_\infty}$, where $k = 0.88$, ρ_∞ and V_∞ are the density and velocity of the solar wind, and D is the areocentric distance to the subsolar point of the magnetosphere. For $D = 4.6 \times 10^3$ km (dimensions of the obstacle estimated above), proton concentration $\rho_\infty \simeq 3$ cm^{-3} and $V_\infty \simeq 400$ km/s, the value of the magnetic moment of Mars $M_m \sim 2 \times 10^{22}$ gauss cm^3.

The magnetic measurements performed on the Mars 2 and Mars 3 satellites by Dolginov et al. (ref. 11) led the authors of these measurements to the conclusion that Mars might have its own magnetic field, and our estimates of the value of magnetic moment do not contradict the estimates of M_m made by Dolginov et al. (ref. 11) on the basis of the magnetic measurements.

One factor in favor of the existence of a Martian magnetosphere is the characteristic variations in the plasma and magnetic field as the spacecraft enter the obstacle. As the Mars 2 and Mars 3 spacecraft crossed the boundary of the obstacle, they observed an increase in the magnetic field modulus along with a drop in the electron flux. This behavior of the plasma and magnetic field is characteristic of the magnetosphere of Earth and non-characteristic of Venus which, apparently, has no magnetic field of its own (the plasma fluxes and magnetic field changed synchronously as Venera 4 approached the surface of Venus (ref. 12).

Let us examine changes in the characteristics of the plasma as Mars 5 entered the obstacle. Figure 3 shows the trajectory sectors of Mars 5 near the planet in coordinates X, $\sqrt{Y^2 + Z^2}$ during two successive revolutions of the satellite around the planet (February 13 and 14, 1974). The roman numerals and various arbitrary symbols show the three characteristic zones intersected by the spacecraft, for which typical spectra are shown in figure 1. The first two zones correspond to the solar wind (fig. 1a) and the transition zone (fig. 1b). Zone III (fig. 1c) corresponds to entry of Mars 5 into the obstacle. For Zone III, a sharp drop in ion currents in comparison with Zones I and II and a decrease in the fluxes of electrons and their temperatures in comparison with Zone II are characteristic. However, the electron currents and temperatures in Zone III are higher than in the unperturbed solar wind in Zone I.

Simultaneous magnetic measurements on Mars 5 (ref. 13) also showed the presence of three zones with mutually different characteristics, for which the boundaries of the zones according to our measurements and the magnetic measurements coincide. On the basis of magnetic data, there were no strong fluctuations of the magnetic field in Zone III, as characteristic of Zone II, and the predominate component of the magnetic field is directed along the Mars-Sun line.

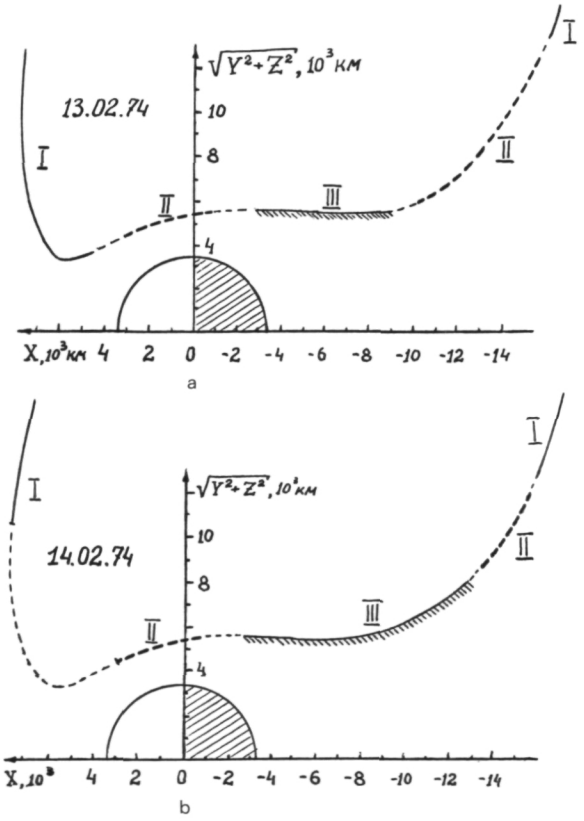

Figure 3.—*The trajectory sectors of Mars 5 near the planet in coordinates X, $\sqrt{Y^2 + Z^2}$ for two successive revolutions of the satellite around the planet (13 and 14 February 1974). The roman numerals and various arbitrary symbols show the three characteristic zones intersected by the spacecraft, for which typical spectra are shown in figure 1.*

Thus, variations in plasma and magnetic field recorded by Mars 5 also indicated that the obstacle at Mars is a magnetosphere, although Mars 5, due to its orbit, apparently recorded the tail of the Martian magnetosphere.

Plasma Zone III bounded by the transition zone behind the bow shock front, may be similar either to the boundary layer in the tail of the terrestrial magnetosphere (ref. 14) or its plasma layer. Comparison of the electron and ion spectra indicates that in this zone the ions are apparently highly isotropic. This allows us to consider Zone III to be more probably a plasma layer in the magnetosphere of Mars rather than its boundary layer. In the boundary layer, as we know from observations near Earth, the essential antisolar component of the directed velocity of the ions is retained. Of course, one should keep in mind the possibility that terrestrial analogues have, in general, little application to the physical phenomena observed on Mars in these experiments, due to essential difference in the relative role of internal and external sources in the Martian magnetic field.

References

1. GRINGAZ, K. I., AND V. V. BEZRUKIKH ET AL., *Kosmich. Issled.*, Vol. 12, 1974, p. 430.
2. DRYER, M., AND G. R. HECKMAN, *Solar Phys.*, Vol. 2, 1967, p. 112.
3. SPREITER, J. R., AND A. Y. ALKSNE, *Rev. of Geophys.*, Vol. 7, 1969, p. 11.
4. GRINGAUZ, K. I., AND V. V. BEZRUKIKH ET AL., *Kosmich. Issled.*, Vol. 12, No. 4., 1974. In press.
5. HESS, W. N., *The Radiation Belt and Magnetosphere*, 1972, p. 216.
6. SPREITER, J. R., AND A. W. RIZZI, *Planet. Sp. Sci.*, Vol. 20, 1972, p. 205.
7. KLIORE, A. J., AND D. L. CAIN ET AL., *Science*, Vol. 149, 1965, p. 1234.
8. KLIORE, A. J., AND G. FJELDBO ET AL., *Science* Vol. 175, 1972, p. 313.
9. KOLOSOV, M. A., AND N. A. SAVICH ET AL., *Radiotekhn. I Electron.*, Vol. 18, 1973, p. 2009.
10. WEISBERG, O. L., AND A. V. BOGDANOV, *Kosmich. Issled.*, Vol. 12, 1974, p. 296.
11. DOLGINOV, SH. SH., YE. G. YEROSHENKO, AND L. N. ZHUZGOV, *DAN SSSR*, Vol. 207, 1972, p. 1296.
12. DOLGINOV, SH. SH., L. N. ZHUZGOV, AND YE. G. YEROSHENKO, *Kosmich. Issled.*, Vol. 6, 1968, p. 561.
13. DOLGINOV, SH. SH., YE. G. YEROSHENKO, L. N. ZHUZGOV, AND V. A. SHAROVA, *The Magnetic Field of Mars According to the Data of the Mars 5 Spacecraft.* This collection, paper 256.
14. ALASOFU, S. I., AND E. W. HONES, JR., ET AL., *J. Geophys. Res.*, Vol. 78, 1973, p. 7257.